



Metformin and cimetidine: Physiologically based pharmacokinetic modelling to investigate transporter mediated drug–drug interactions



H.J. Burt^{a,*}, S. Neuhoff^a, L. Almond^a, L. Gaohua^a, M.D. Harwood^a, M. Jamei^a, A. Rostami-Hodjegan^{a,b}, G.T. Tucker^c, K. Rowland-Yeo^a

^a Simcyp (a Certara Company), Sheffield, UK

^b Manchester Pharmacy School, Faculty of Medical and Human Sciences, University of Manchester, Manchester, UK

^c Medicine and Biomedical Sciences (emeritus), University of Sheffield, Sheffield, UK

ARTICLE INFO

Article history:

Received 13 November 2015

Received in revised form 10 February 2016

Accepted 22 March 2016

Available online 25 March 2016

Keywords:

PBPK

IVIVE

Drug transporters

Drug–drug interactions

ABSTRACT

Metformin is used as a probe for OCT2 mediated transport when investigating possible DDIs with new chemical entities. The aim of the current study was to investigate the ability of physiologically-based pharmacokinetic (PBPK) models to simulate the effects of OCT and MATE inhibition by cimetidine on metformin kinetics. PBPK models were developed, incorporating mechanistic kidney and liver sub-models for metformin (OCT and MATE substrate) and a mechanistic kidney sub-model for cimetidine. The models were used to simulate inhibition of the MATE1, MATE2-K, OCT1 and OCT2 mediated transport of metformin by cimetidine. Assuming competitive inhibition and using cimetidine K_i values determined *in vitro*, the predicted metformin AUC ratio was 1.0 compared to an observed value of 1.46. The observed AUC ratio could only be recovered with this model when the cimetidine K_i for OCT2 was decreased 1000-fold or the K_i 's for both OCT1 and OCT2 were decreased 500-fold. An alternative description of metformin renal transport by OCT1 and OCT2, incorporating electrochemical modulation of the rate of metformin uptake together with 8–18-fold decreases in cimetidine K_i 's for OCTs and MATEs, allowed recovery of the extent of the observed effect of cimetidine on metformin AUC. While the final PBPK model has limitations, it demonstrates the benefit of allowing for the complexities of passive permeability combined with active cellular uptake modulated by an electrochemical gradient and active efflux.

© 2016 Simcyp Limited. Published by Elsevier B.V. This is an open access article under the CC BY license (<http://creativecommons.org/licenses/by/4.0/>).

1. Introduction

Metformin is widely prescribed as a first-line therapy for type II diabetes mellitus. As it is a hydrophilic base present in its cationic form at

Abbreviations: AUC, area under the plasma concentration–time curve; B/P, blood-to-plasma ratio; CYP, cytochrome P450; CL_{int} , intrinsic clearance; C_{max} , maximum plasma concentration; CL_{PD} , passive permeability–surface area product; DDI, drug–drug interaction; f_a , fraction absorbed; J_{max} , maximum rate of active transport; J_{OCT1} , rate of OCT1 transport; J_{OCT2} , rate of OCT2 transport; k_a , absorption rate constant; K_i , inhibition constant; K_m , Michaelis constant; K_p , tissue to plasma partition coefficient; MATE, multidrug and toxin extrusion protein; Mech KiM, mechanistic kidney model; OAT, organic anion transporter; OCT, organic cation transporter; PE, parameter estimation; PerL, permeability-limited liver model; PMAT, plasma membrane monoamine transporter; PTC, proximal tubule cells; RAF, relative activity factor; t_{lag} , time-lag; t_{max} , time of maximum plasma concentration; V_{ss} , volume of distribution at steady-state; Φ_{dr} , electrochemical driving force; Φ_m , membrane potential.

* Corresponding author at: Simcyp Limited, Blades Enterprise Centre, John Street, Sheffield S2 4SU, UK.

E-mail addresses: Howard.burt@certara.com (H.J. Burt), Sibylle.neuhoff@certara.com (S. Neuhoff), Lisa.almond@certara.com (L. Almond), Gaohua.lu@certara.com (L. Gaohua), Matthew.harwood@certara.com (M.D. Harwood), Masoud.Jamei@certara.com (M. Jamei), Amin.rostami@manchester.ac.uk (A. Rostami-Hodjegan), G.t.tucker@sheffield.ac.uk (G.T. Tucker), Karen.yeo@certara.com (K. Rowland-Yeo).

physiological pH, its pharmacokinetic behaviour is dictated largely by the influence of transporters (Graham et al., 2011). The physicochemical properties of metformin also determine that its elimination is predominantly by renal excretion (80%), with a minor contribution from metabolism (Sirtori et al., 1978; Tucker et al., 1981). While the magnitudes of documented drug–drug interactions (DDIs) affecting metformin as a victim are not of major clinical significance, the compound is recommended by the US FDA as a probe for OCT2 mediated transport when investigating possible DDIs with new chemical entities (U.S. Department of Health and Human Services et al., 2012). On this basis, a sound mechanistic understanding of DDIs with metformin is important. Such DDIs, involving raised drug exposure in the kidney, are not necessarily reflected in an equivalent change in systemic exposure (Sprowl and Sparreboom, 2014).

Within the proximal tubule cells of the kidney, metformin is actively transported across the basal membrane by OCT2 and effluxed into the tubular fluid at the apical membrane by MATE1 and MATE2-K (Koepsell et al., 2007; Pelis and Wright, 2011). In hepatocytes it has been shown to be a substrate for OCT1 expressed on the sinusoidal membrane (Koepsell, 2011). Although MATE1 is expressed on the canalicular membrane of hepatocytes, biliary clearance of metformin is

negligible (Tucker et al., 1981). In the gut wall, paracellular transfer appears to be significant (Proctor et al., 2008), while metformin has also been shown to be a substrate for OCT1, OCT3 and PMAT at the apical membrane of enterocytes (Muller et al., 2005; Zhou et al., 2007). Metabolism of metformin by CYP3A4 has been reported based on studies with recombinant enzyme (Choi et al., 2010).

Co-administration of cimetidine, pyrimethamine, trimethoprim, lansoprazole, dolutegravir and vandetanib with metformin has been shown to increase its AUC by 1.2 to 1.7-fold (Ding et al., 2014; Grun et al., 2013; Johansson et al., 2014; Kusuhara et al., 2011; Somogyi et al., 1987; Wang et al., 2008; Zong et al., 2014). All of these compounds are inhibitors of OCT2, while cimetidine, pyrimethamine and trimethoprim are also reported to be inhibitors of MATE transporters. Cimetidine K_i values for MATE1 and MATE2-K are, respectively, 62- and 40-fold lower than those for OCT2 inhibition, suggesting that the latter is unlikely to be significant after therapeutic doses of cimetidine (Ito et al., 2012; Tsuda et al., 2009). Similarly, pyrimethamine K_i values for MATE1 and MATE2-K are 118- and 193-fold lower than those for OCT2 inhibition, respectively (Ito et al., 2010; Kusuhara et al., 2011).

The incorporation of permeability-limited uptake models within conventional PBPK models has been shown to improve insight into transporter mediated DDIs in the liver (Li et al., 2014). However, examples where this approach has been used to simulate transporter mediated DDIs in the kidney are rare. Posada et al. (2015) used a mechanistic kidney model to simulate the increase in pemetrexed exposure due to inhibition of renal OAT3 uptake by ibuprofen. Hsu et al. (2014) investigated DDIs between probenecid and three renally cleared drugs using a similar approach. However, *in vitro* data for the inhibition of specific transporters by probenecid were not applied, obscuring understanding of the impact of the relative inhibition of uptake and efflux transporters. In addition, permeability-limited PBPK models typically assume that active transport will follow first-order or Michaelis–Menten kinetics, with little acknowledgement of the mechanism(s) of transport. The driving force for transport varies greatly amongst the known drug transporters. For example, despite OCT and MATE both being solute carriers, transport by the former is driven by the electrochemical gradient across the cell membrane while the latter is an antiporter of protons (Pelis and Wright, 2011).

We describe an attempt to simulate reported effects of cimetidine on the kinetics of metformin using a PBPK model incorporating active uptake and efflux in the kidney and permeability-limited uptake in the liver based on available *in vitro* and *in vivo* data. A novel feature of the final model for metformin was the incorporation of an electrochemical driving force for uptake by OCT1 and OCT2.

2. Material and methods

Full PBPK models were developed for metformin and cimetidine in the Simcyp Simulator® Version 14 (Simcyp Ltd., A Certara Company, Sheffield, UK) (Fig. 1). For metformin, renal and hepatic disposition were described by a mechanistic kidney model (Mech KiM) (Neuhoff et al., 2013a) and a permeability-limited liver model (PerL) (Jamei et al., 2014; Neuhoff et al., 2013b), respectively. For cimetidine, renal disposition was described by Mech KiM. For both compounds, distribution to all other organs was assumed to be perfusion-limited, with tissue-to-plasma partition coefficients (K_p 's) predicted using the method of Rodgers et al. (Jamei et al., 2014; Rodgers and Rowland, 2007). A schematic representation of the processes governing the renal secretion of metformin and cimetidine in the proximal tubule of the kidney is shown in Fig. 2.

2.1. Model development

2.1.1. Metformin

Data used in the development of the metformin model are summarised in Table 1. Where these data were obtained from more

than one study, weighted mean values were calculated based on the number of observations in each study. Absorption following an oral dose of metformin was described as a first-order process after a lag time (t_{lag}) with a mean fraction absorbed (f_a) of 0.7 (Pentikainen et al., 1979; Tucker et al., 1981). Estimates of k_a were obtained by fitting a one-compartment PK model to mean plasma metformin concentrations reported after administration of 500 to 1500 mg immediate release tablets using Phoenix® WinNonlin® software (Version 6.3, Pharsight, A Certara Company). A weighted mean value of k_a was determined based on the number of individuals in each study.

Total metabolic clearance in the liver was incorporated in the model based on back calculation of intrinsic metabolic clearance from the total blood clearance after an intravenous dose ($32.0 \text{ L} \cdot \text{h}^{-1}$) after subtraction of renal clearance with respect to blood ($26.1 \text{ L} \cdot \text{h}^{-1}$), using the method described by Jamei et al. (2014) (Jamei et al., 2014; Pentikainen et al., 1979; Sirtori et al., 1978; Tucker et al., 1981). A fixed average blood-to-plasma ratio of metformin was determined from paired AUC values in blood and plasma after intravenous and oral dosing (Robert et al., 2003; Sambol et al., 1995; Tucker et al., 1981).

The steady state volume of distribution of metformin (V_{ss}) was predicted using the method of Rodgers and Rowland (2007).

Data describing the OCT2, MATE1 and MATE2-K mediated transport of metformin were obtained from a study using transfected HEK293 cells (Ito et al., 2012). Rates of transport were extracted from Eadie–Hofstee plots and converted from units of $\mu\text{L} \cdot \text{min}^{-1} \cdot \text{mg protein}^{-1}$ to $\mu\text{L} \cdot \text{min}^{-1} \cdot 10^6 \text{ cells}^{-1}$ on the basis that 1 million HEK293 cells contain 0.93 mg of total protein (Lazorova, 2010). Estimates of the maximum rate of active transport (J_{max}), Michaelis constant (K_m) and the passive permeability-surface area product (CL_{PD}) were obtained by nonlinear least squares regression using Equation 1. As saturation of transport was not observed at therapeutic concentrations ($K_m > 300 \mu\text{M}$ in all cases) intrinsic clearances ($\mu\text{L} \cdot \text{min}^{-1} \cdot 10^6 \text{ PTC}^{-1}$) for OCT2 uptake and the sum of MATE1 and MATE2-K (MATE1/2-K) efflux were applied in Mech KiM.

$$\text{uptake rate} = \frac{J_{max} \cdot [S]}{K_m + [S]} + CL_{PD} \cdot [S] \quad (1)$$

where the rate of uptake is in units of $\text{pmol} \cdot \text{min}^{-1} \cdot 10^6 \text{ cells}^{-1}$, $[S]$ is the substrate concentration (μM), J_{max} is the maximum rate of active transport ($\text{pmol} \cdot \text{min}^{-1} \cdot 10^6 \text{ cells}^{-1}$), K_m is the Michaelis constant (μM) and CL_{PD} is the passive permeability-surface area product ($\mu\text{L} \cdot \text{min}^{-1} \cdot 10^6 \text{ cells}^{-1}$).

The passive permeability of metformin in the kidney ($CL_{PD, \text{kidney}}$) was obtained by multiplying permeability in a PAMPA system ($5 \times 10^{-7} \text{ cm} \cdot \text{s}^{-1}$ (Balimane and Chong, 2008)) by an estimated total nephron surface area. In Mech KiM, the lengths and diameters of the proximal tubule, loop of Henle, distal tubule and collecting duct are defined for a typical nephron (Neuhoff et al., 2013a). From these, the surface area of a single nephron was calculated and scaled to a total nephron surface area of 291 cm^2 based on the number of nephrons (1.6×10^6) in a representative healthy Caucasian (Neuhoff et al., 2013a).

Hepatic uptake by OCT1 and passive permeability in the liver were applied in the PerL model using estimates of intrinsic clearance and $CL_{PD, \text{liver}}$, respectively, from experiments with cryopreserved human hepatocytes (Sogame et al., 2009).

To account for discrepancies in both transporter expression and activity between *in vitro* transfection systems and *in vivo* proximal tubule cells/hepatocytes, relative activity factors (RAFs) were estimated as scalars for each active transport process (Harwood et al., 2013). Currently, experimental RAF values for the relevant transporters are not available. Therefore, operational values were determined by fitting a training set of mean plasma drug concentration-time and urinary excretion data collated from one study in which a 250 mg intravenous bolus dose of metformin was administered (Tucker et al., 1981) and three studies in which 500 mg oral doses (Caille et al., 1993; Karttunen et al., 1983;

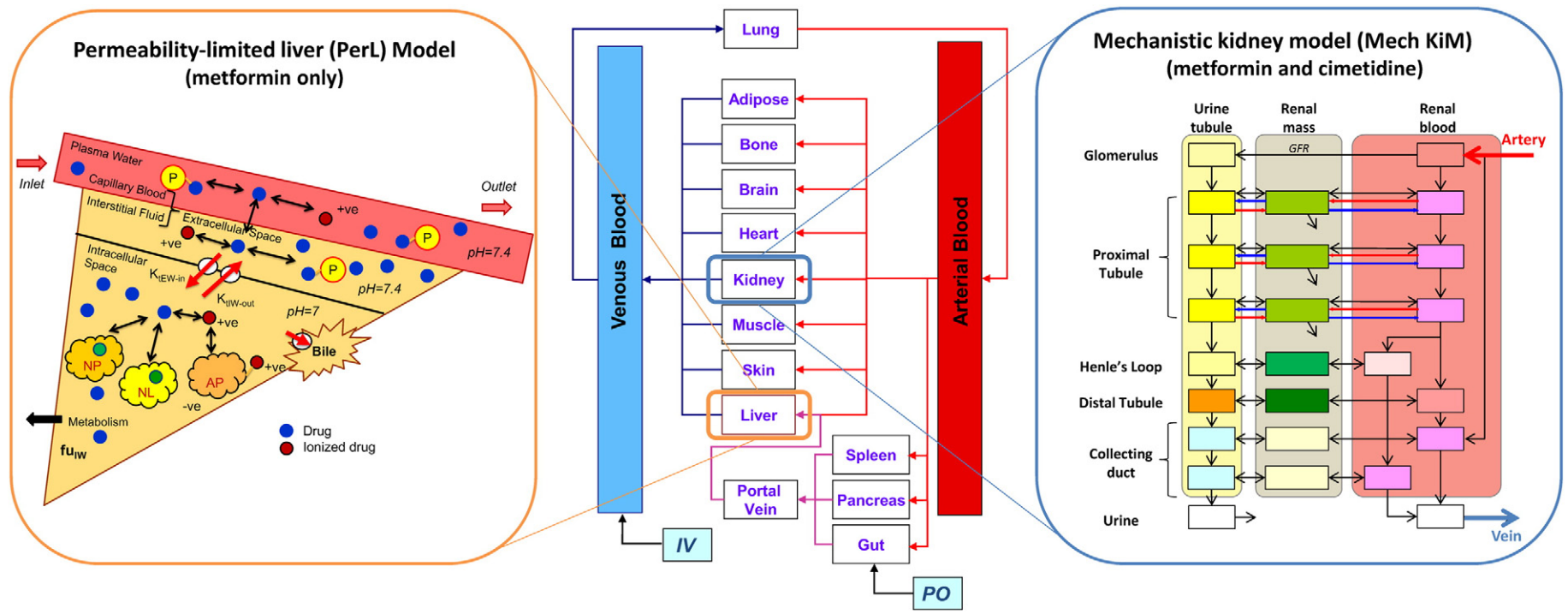


Fig. 1. Structure of a general PBPK model used to describe the kinetics of metformin and cimetidine (centre) and associated nested permeability-limited liver (PerL, left) and mechanistic kidney (Mech KiM, right) models.

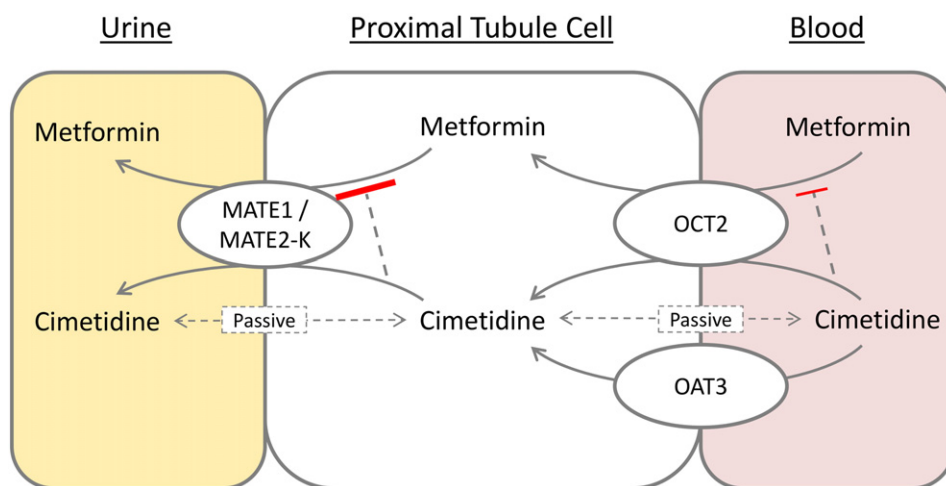


Fig. 2. A schematic representation of transport processes for metformin and cimetidine and their interaction in renal proximal tubule cells.

Sambol et al., 1996a) were given. RAF values were determined sequentially for each transporter and, in each case, studies were fitted individually and a mean RAF was applied in the model. Firstly, a RAF value for OCT1 transport in the liver was determined by fitting the *in vivo* plasma

data using the parameter estimation module within the Simcyp Simulator (weighted least squares fitting, weighted by the reciprocal of the predicted value squared), while fixing metformin renal clearance at the observed mean value of $26.1 \text{ L} \cdot \text{h}^{-1}$ (Pentikainen et al., 1979;

Table 1

Parameter values used to construct the PBPK model for metformin.

Parameter	Value (%CV)	Source	Comments
Physchem and blood binding			
Molecular weight	129.16		
Compound type	Monoprotic base		
pKa	11.8	Avdeef (2012), Ray (1961)	Measured
LogP	−1.43	Schafer and Bojanowski, (1972)	Measured
fu	1	Tucker et al. (1981)	Measured
B/P	1	Robert et al. (2003), Sambol et al. (1995), Tucker et al. (1981)	Calculated from $\text{AUC}_{\text{blood}}/\text{AUC}_{\text{plasma}}$
Absorption			
ka (h^{-1})	0.27 (30)	Caille et al. (1993), Chen et al. (2009); Pentikainen et al. (1979), Sambol et al. (1996a), Sambol et al. (1995), Sambol et al. (1996b)	Fitted
t _{lag} (h)	0.29 (56)	Tucker et al. (1981)	Fitted
f _a	0.7 (16)	Pentikainen et al. (1979), Tucker et al. (1981)	Value from <i>in vivo</i> data
Distribution			
Model	Full PBPK		
V _{ss} (L/kg)	0.99		Predicted – Rodgers and Rowland method (Rodgers and Rowland, 2007)
Transport-kidney			
Model	Mech KiM		
OCT2 CL _{int} ($\mu\text{L} \cdot \text{min}^{-1} \cdot 10^6 \text{ PTC}^{-1}$)	14.2	Ito et al. (2012)	Measured-transfected HEK293
OCT2 RAF	3		Fitted
MATE1/MATE2-K CL _{int} ($\mu\text{L} \cdot \text{min}^{-1} \cdot 10^6 \text{ PTC}^{-1}$)	16.6	Ito et al. (2012)	Measured-transfected HEK293
MATE1/MATE2-K RAF	3		Fitted
CL _{PD,kidney} ($\text{mL} \cdot \text{min}^{-1} \cdot 10^6 \text{ PTC}^{-1}$)	4.26×10^{-7}	Balimane and Chong (2008)	Scaled PAMPA permeability
f _{u,kidney cell}	1		Predicted – Rodgers and Rowland method (Rodgers and Rowland, 2007)
Transport-liver			
Model	PerL		
OCT1 CL _{int} ($\mu\text{L} \cdot \text{min}^{-1} \cdot 10^6 \text{ hepatocytes}^{-1}$)	0.316	Sogame et al. (2009)	Measured – cryopreserved hepatocytes
OCT1 RAF	3		Fitted
CL _{PD,liver} ($\text{mL} \cdot \text{min}^{-1} \cdot 10^6 \text{ hepatocytes}^{-1}$)	5.88×10^{-5}	Sogame et al. (2009)	Measured – cryopreserved hepatocytes
f _{u,hepatocyte}	1		Predicted – Rodgers and Rowland method (Rodgers and Rowland, 2007)
Metabolism			
HLM CL _{int} ($\mu\text{L} \cdot \text{min}^{-1} \cdot \text{mg protein}^{-1}$)	1.62	Pentikainen et al. (1979), Sirtori et al. (1978), Tucker et al. (1981)	Retrograde calculation

Sirtori et al., 1978; Tucker et al., 1981). Secondly, using Mech KiM and the resulting hepatic OCT1 RAF, the RAF for OCT2 uptake in the kidney was obtained by fitting of the plasma metformin concentration data. Finally, a RAF value for MATE1/2-K efflux in the kidney was obtained by sensitivity analysis of the urinary excretion data.

2.1.2. Cimetidine

Data used in the development of the cimetidine model are summarised in Table 2. Absorption following an oral dose of cimetidine was described by a first-order process after a lag time (t_{lag}). Estimates for k_a and t_{lag} were obtained by fitting plasma cimetidine drug concentration-time profiles reported after the administration of 400 mg cimetidine as immediate release tablets (Grahnen et al., 1979; Gugler et al., 1981a; Somogyi et al., 1981) with the cimetidine PBPK model using the parameter estimation module within the Simcyp Simulator (weighted least squares fitting, weighted by the reciprocal of the predicted value squared). Total metabolic clearance in the liver was incorporated in the model by back-calculation of intrinsic metabolic clearance from total blood clearance following an intravenous dose (41.0 L/

h) after subtraction of renal clearance with respect to blood (32.6 L/h), using the retrograde calculation method described by Jamei et al. (2014) (Grahnen et al., 1979; Jamei et al., 2014; Lebert et al., 1981; Somogyi and Gugler, 1985; Villeneuve et al., 1983; Walkenstein et al., 1978).

The volume of distribution of cimetidine (V_{ss}) was predicted using the method of Rodgers and Rowland (2007).

Data describing the OAT3, OCT2, MATE1 and MATE2-K mediated uptake of cimetidine were obtained from studies using transfected HEK293 cells (Erdman et al., 2006; Ito et al., 2012; Matsumoto et al., 2008; Ohta et al., 2009; Tahara et al., 2005). In addition, K_i values for OCT1, OCT2, MATE1 and MATE2-K inhibitions by cimetidine in HEK293 cells were utilised to predict the interaction with metformin (Ito et al., 2012). As the K_i values for MATE1 and MATE2-K were within 1.8-fold of each other, an average value was applied with respect to a combined metformin MATE1/2-K intrinsic clearance (Ito et al., 2012). The $CL_{PD,kidney}$ of cimetidine applied within Mech KiM was obtained by multiplying Caco-2 permeability ($3 \times 10^{-5} \text{ cm} \cdot \text{s}^{-1}$ (Balimane and Chong, 2008)) by the total nephron surface area as described for

Table 2
Parameter values used to construct the PBPK model for cimetidine.

Parameter	Value (%CV)	Source	Comments
Physchem and blood binding			
Molecular weight	252.34		
Compound type	Monoprotic base		
pKa	6.9	Avdeef and Berger (2001), Durant et al. (1977)	Measured
LogP	0.48	Avdeef and Berger (2001)	Measured
f_u	0.8	Somogyi et al. (1980), Taylor et al. (1978)	Measured
B/P	0.97	Somogyi et al. (1980)	Measured
Absorption			
k_a (h^{-1})	0.7 (18)	Grahnen et al. (1979), Gugler et al. (1981a), Somogyi et al. (1981)	Fitted
t_{lag} (h)	0.15 (28)	Grahnen et al. (1979), Gugler et al. (1981a), Somogyi et al. (1981)	Fitted
f_a	0.92 (30)	Gugler et al. (1981b), Taylor et al. (1978)	Value from <i>in vivo</i> data
Distribution			
Model	Full PBPK		
V_{ss} (L/kg)	0.60		Predicted – Rodgers and Rowland method (Rodgers and Rowland, 2007)
Transport-kidney			
Model	Mech KiM		
OCT2 J_{max} ($\text{pmol} \cdot \text{min}^{-1} \cdot 10^6$ PTC $^{-1}$)	2170	Tahara et al. (2005)	Measured – transfected HEK293
OCT2 K_m (μM)	72.6	Tahara et al. (2005)	Measured – transfected HEK293
OCT2 RAF	3		Same as value for metformin
OAT3 J_{max} ($\text{pmol} \cdot \text{min}^{-1} \cdot 10^6$ PTC $^{-1}$)	1232	Erdman et al. (2006), Tahara et al. (2005)	Measured – transfected HEK293
OAT3 K_m (μM)	161.5	Erdman et al. (2006), Tahara et al. (2005)	Measured – transfected HEK293
OAT3 RAF	3		Same as value for metformin
MATE1 J_{max} ($\text{pmol} \cdot \text{min}^{-1} \cdot 10^6$ PTC $^{-1}$)	135.5	Matsumoto et al. (2008), Ohta et al. (2009)	Measured – transfected HEK293
MATE1 K_m (μM)	7.7	Matsumoto et al. (2008), Ohta et al. (2009)	Measured – transfected HEK293
MATE1 RAF	3		Same as value for metformin
MATE2-K J_{max} ($\text{pmol} \cdot \text{min}^{-1} \cdot 10^6$ PTC $^{-1}$)	216	Ohta et al. (2009)	Measured – transfected HEK293
MATE2-K K_m (μM)	18.2	Ohta et al. (2009)	Measured – transfected HEK293
MATE2-K RAF	3		Same as value for metformin
OCT1 K_i (μM)	104	Ito et al. (2012)	Measured – transfected HEK293
OCT2 K_i (μM)	124	Ito et al. (2012)	Measured – transfected HEK293
MATE1/MATE2-K K_i (μM)	5.4	Ito et al. (2012)	Measured – mean of MATE1 and MATE2K
$CL_{PD,kidney}$ ($\text{mL} \cdot \text{min}^{-1} \cdot 10^6$ PTC $^{-1}$)	2.61×10^{-5}	Balimane and Chong, (2008)	Scaled from Caco-2 permeability
$f_{u,kidney \text{ cell}}$	1		Predicted – Rodgers and Rowland method (Rodgers and Rowland, 2007)
Metabolism			
HLM CL_{int} ($\mu\text{L} \cdot \text{min}^{-1} \cdot \text{mg}$ protein $^{-1}$)	2.87	Grahnen et al. (1979), Lebert et al. (1981), Somogyi and Gugler (1985), Villeneuve et al. (1983), Walkenstein et al. (1978)	Retrograde calculation

metformin. The operational RAF values estimated for metformin were also applied for cimetidine. This was done on the basis that the parameters describing the OCT2/MATE transport of cimetidine and metformin were both derived from studies with transfected HEK293 cells and in 3 out of 4 cases the cimetidine *in vitro* data were obtained from the same laboratory. With respect to the OAT3 RAF for cimetidine, the assumption was made that the similarity in the determined RAF values for OCT2 and MATEs in transfected HEK293 cells extended to this transporter.

2.2. Model verification

The performance of the metformin and cimetidine PBPK models was evaluated by comparing simulated plasma drug concentrations and urinary excretion rates with those observed in a test set of studies not used to build the model. For metformin, its kinetics after single 500–1500 mg oral doses and 500 mg BID oral doses was simulated (Balan et al., 2001; Gusler et al., 2001; Karttunen et al., 1983; Pentikainen, 1986; Scheen et al., 1994; Tucker et al., 1981; Tzvetkov et al., 2009). For cimetidine, its kinetics after single 300 mg oral doses and multiple 400 mg BID and TID oral doses was simulated (Kirch et al., 1989; Muirhead et al., 1986; Somogyi et al., 1987; Walkenstein et al., 1978). Data from two studies involving the co-administration of metformin (250 mg QD and 500 mg single dose) and cimetidine (400 mg BID) were also simulated (Somogyi et al., 1987; Wang et al., 2008). For each study, ten trials were simulated in which the number, age range and gender of the virtual subjects were matched to those of the real subjects. The ‘Sim-Healthy Volunteer’ population library was used to simulate trials conducted in healthy Caucasian subjects and the ‘Chinese-Healthy Volunteer’ population library was used to simulate the DDI study of Wang et al., 2008. In the latter study, mean plasma metformin concentrations and PK parameters were reported for different genotypes of the OCT2 808G > T variant. In this case, population mean values were generated using the expected number of individuals with each genotype, based on the allele frequency reported in the study and assuming Hardy–Weinberg equilibrium.

A sensitivity analysis was performed to investigate the impact of decreasing the cimetidine K_i values for OCT1, OCT2 and MATE1/2-K determined *in vitro*. This was done using a single virtual healthy subject with the mean attributes of the Caucasian population.

2.3. Model refinement

An alternative description of metformin transport by OCT1 and OCT2 was devised, accounting for modulation of these processes by an electrochemical driving force (Φ_{df}). As the intracellular to extracellular drug concentration ratio increases, this electrochemical driving force decreases, thereby placing a feedback limit on the extent of intracellular accumulation. In the first instance, the data of Kimura et al. (2005) and Nies et al. (2011) on the uptake of metformin into HEK293 cells transfected with OCT2 and OCT1, respectively, were fitted by a two compartment model defining drug concentration in the incubation medium (Equation 2) and in the cells (Equation 3), using the R programming language (Version 3.0.1, R Foundation for Statistical Computing). Φ_{df} is defined as the difference between the membrane potential (Φ_m) and the ion equilibrium potential described by the Nernst equation (Equation 4). It has a negative value when conditions favour the uptake of metformin into the cell. Passive transcellular movement of metformin was assumed to be negligible on the basis of negligible accumulation in non-transfected HEK293 cells.

$$V_{med} \cdot \frac{d[S]_{med}}{dt} = \Phi_{df} \cdot J_{OCT} \cdot \text{No. cells} \quad (2)$$

$$V_{cell} \cdot \text{No. cells} \cdot \frac{d[S]_{cell}}{dt} = -\Phi_{df} \cdot J_{OCT} \cdot \text{No. cells} \quad (3)$$

where $[S]_{med}$ and $[S]_{cell}$ are the substrate concentrations (μM) in medium and cells, respectively; V_{med} and V_{cell} are the volume (μL) of the medium and cells (per 10^6 cells), respectively; J_{OCT} is the rate ($\text{pmol} \cdot \text{min}^{-1} \cdot \text{volt}^{-1} \cdot 10^6 \text{ cells}^{-1}$) of OCT1 or OCT2 mediated transport; No. cells is the number of cells (10^6 cells) in the monolayer and Φ_{df} is the electrochemical driving force (volts).

$$\Phi_{df} = \Phi_m - \frac{R \cdot T}{z \cdot F} \cdot \ln \left(\frac{[S]_{med} \cdot f_{u_{med}}}{[S]_{cell} \cdot f_{u_{cell}}} \right) \quad (4)$$

where Φ_m is the membrane potential (volts), R is the universal gas constant ($8.314 \text{ J} \cdot \text{K}^{-1} \cdot \text{mol}^{-1}$), T is temperature (310.15 K in the experiment at 37 °C), z is the valence of the ionic species (1 for metformin), F is Faraday’s constant ($96,490 \text{ C} \cdot \text{mol}^{-1}$) and $f_{u_{med}}$ and $f_{u_{cell}}$ are the fractions of metformin unbound in media and cells, respectively (both assumed to be 1).

The number of cells in the HEK293-OCT2 and HEK293-OCT1 monolayers were estimated to be 1.73×10^6 and 1.68×10^6 , respectively, based on the seeding densities and the growth rate of HEK293 monolayers over the culture period (Park et al., 2004). A HEK293 cell volume of $6.4 \mu\text{L}/\text{mg}$ protein was used (Gillen and Forbush, 1999; Tamai et al., 1997). This equates to a total cell volumes (V_{cell}) of $10.2 \mu\text{L}$ and $10.1 \mu\text{L}$ for the HEK293-OCT2 and HEK293-OCT1 monolayers, respectively, given that 1 million HEK293 cells contain 0.93 mg of total protein (Lazorova, 2010). A Φ_m value of -35 mV was used based on data obtained with non-transfected HEK293 cells (Chemin et al., 2000).

With all other parameters fixed, the value of J_{OCT} was determined by weighted ($1/Y^2$) least squares regression using the ‘optim’ function (L-BFGS-B method) in R. A corresponding value of $CL_{int,OCT2}$ based on a conventional uptake function was determined by fitting Equations 5 and 6.

$$V_{med} \cdot \frac{d[S]_{med}}{dt} = -CL_{int,OCT} \cdot \text{No. cells} \cdot [S]_{med} \cdot f_{u_{med}} \quad (5)$$

$$V_{cell} \cdot \text{No. cells} \cdot \frac{d[S]_{cell}}{dt} = CL_{int,OCT} \cdot \text{No. cells} \cdot [S]_{med} \cdot f_{u_{med}} \quad (6)$$

where $CL_{int,OCT}$ is the intrinsic clearance ($\mu\text{L} \cdot \text{min}^{-1} \cdot 10^6 \text{ cells}^{-1}$) for OCT mediated transport.

The impact of incorporating the electrogenic OCT1 and OCT2 transport models into the PBPK model for metformin was evaluated. For this purpose, the previously described PBPK models for metformin and cimetidine were recreated in Simulink (Version 8.1; MathWorks, Inc., Natick, MA) with the rate of OCT1 mediated uptake of metformin from extracellular water into hepatocytes defined either by Equation 7 (conventional model) or Equations 9 and 10 (electrogenic model) and the rate of OCT2 mediated uptake of metformin from blood into proximal tubule cells defined either by Equation 8 (conventional model) or Equations 11 and 12 (electrogenic model). The relevant J_{OCT} for use with the electrogenic model was the value obtained by fitting the *in vitro* data.

$$\begin{aligned} \text{rate of OCT1 uptake} \\ = [\text{Metformin}]_{EW,u} \cdot \frac{CL_{int,OCT1}}{1 + \frac{[\text{Cimetidine}]_{B,u}}{K_{i,OCT1}}} \cdot \text{RAF} \cdot \text{HPGL} \cdot \text{LW} \cdot 60 / 10^6 \end{aligned} \quad (7)$$

where the rate of OCT1 uptake is the value for the whole liver ($\mu\text{mol}/\text{h}$); $CL_{int,OCT1}$ is the *in vitro* intrinsic clearance for OCT1 uptake ($\mu\text{L} \cdot \text{min}^{-1} \cdot 10^6 \text{ cells}^{-1}$); $[\text{Metformin}]_{EW,u}$ and $[\text{Cimetidine}]_{B,u}$ are the unbound concentrations of metformin and cimetidine, respectively in hepatic extracellular water and blood (μM); $K_{i,OCT1}$ is the cimetidine OCT1 inhibition constant (μM); HPGL is hepatocytes per gram of liver

(10^6 cells) and LW is the liver weight (grams).

rate of OCT2 uptake

$$= [\text{Metformin}]_{\text{PT},\text{B},\text{u}} \cdot \frac{\text{CL}_{\text{int},\text{OCT2}}}{1 + \frac{[\text{Cimetidine}]_{\text{PT},\text{B},\text{u}}}{K_{i,\text{OCT2}}}} \cdot \text{RAF} \cdot \text{PTCPGK} \cdot \text{KW} \cdot 60 / 10^6 \quad (8)$$

where the rate of OCT2 uptake is the value for both kidneys ($\mu\text{mol}/\text{h}$); $\text{CL}_{\text{int},\text{OCT2}}$ is the *in vitro* intrinsic clearance for OCT2 uptake ($\mu\text{L} \cdot \text{min}^{-1} \cdot 10^6 \text{ cells}^{-1}$); $[\text{Metformin}]_{\text{PT},\text{B},\text{u}}$ and $[\text{Cimetidine}]_{\text{PT},\text{B},\text{u}}$ are the unbound concentrations of metformin and cimetidine, respectively in proximal tubule blood (μM); $K_{i,\text{OCT2}}$ is the cimetidine OCT2 inhibition constant (μM); PTCPGK is proximal tubule cells per gram of kidney (10^6 cells) and KW is the weight of both kidneys (grams).

rate of OCT1 uptake

$$= -\phi_{\text{df}} \cdot \frac{J_{\text{OCT1}}}{1 + \frac{[\text{Cimetidine}]_{\text{B},\text{u}}}{K_{i,\text{OCT1}}}} \cdot \text{RAF} \cdot \text{HPGL} \cdot \text{LW} \cdot 60 / 10^6 \quad (9)$$

$$\phi_{\text{df}} = \phi_m - \frac{R \cdot T}{z \cdot F} \cdot \ln \left(\frac{[\text{Metformin}]_{\text{EW},\text{u}}}{[\text{Metformin}]_{\text{IW},\text{u}}} \right) \quad (10)$$

where J_{OCT1} is the *in vitro* rate of OCT1 uptake ($\text{pmol} \cdot \text{min}^{-1} \cdot \text{volt}^{-1} \cdot 10^6 \text{ cells}^{-1}$) and $[\text{Metformin}]_{\text{IW},\text{u}}$ is the unbound concentration of metformin in intracellular water of hepatocytes. A ϕ_m for hepatocytes of -35 mV was used (Veech et al., 1995).

rate of OCT2 uptake

$$= -\phi_{\text{df}} \cdot \frac{J_{\text{OCT2}}}{1 + \frac{[\text{Cimetidine}]_{\text{PT},\text{B},\text{u}}}{K_{i,\text{OCT2}}}} \cdot \text{RAF} \cdot \text{PTCPGK} \cdot \text{KW} \cdot 60 / 10^6 \quad (11)$$

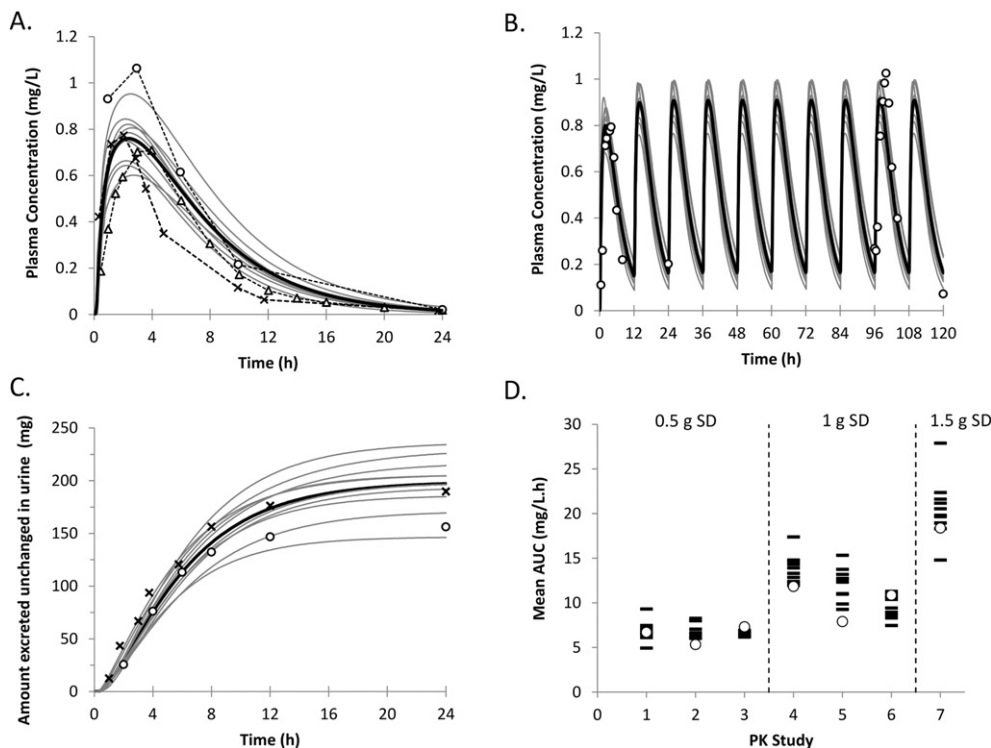


Fig. 3. Comparison of mean simulated plasma metformin concentrations (black line) and observed data after (A) a single 500 mg dose (X = Tucker et al., 1981, Δ = Gusler et al., 2001, O = Tzvetkov et al., 2009), (B) 500 mg BID dosing (O = Karttunen et al., 1983). (C) Comparison of mean simulated urinary recovery of unchanged metformin in urine (black line) and observed data after a single 500 mg dose (X = Tucker et al., 1981, O = Karttunen et al., 1983). Grey lines represent the mean data for each of 10 simulated trials. (D) Comparison of simulated (10 trials) (—) and observed (O) mean metformin single dose AUC values. PK studies: 1 and 7, (Tucker et al., 1981); 2, (Gusler et al., 2001); 3, (Tzvetkov et al., 2009); 4, (Balan et al., 2001); 5, (Pentikainen, 1986); 6, (Scheen et al., 1994); 8, (Karttunen et al., 1983).

$$\phi_{\text{df}} = \phi_m - \frac{R \cdot T}{z \cdot F} \cdot \ln \left(\frac{[\text{Metformin}]_{\text{PT},\text{B}} \cdot \frac{f_u}{B/P}}{[\text{Metformin}]_{\text{PT},\text{cell}} \cdot f_{u,\text{kidney cell}}} \right) \quad (12)$$

where J_{OCT2} is the *in vitro* rate of OCT2 uptake ($\text{pmol} \cdot \text{min}^{-1} \cdot \text{volt}^{-1} \cdot 10^6 \text{ cells}^{-1}$) and $f_{u,\text{kidney cell}}$ is the free fraction of drug in the kidney cell. A ϕ_m for proximal tubule cells of -60 mV was used (Pelis and Wright, 2011).

Following the incorporation of the electrogenic equations into the PBPK model for metformin, the RAF values for OCT1, OCT2 and MATEs were simultaneously re-optimised using plasma and urinary excretion data from the metformin training dataset described previously. This model was used to simulate the effects of cimetidine (400 mg BID) on metformin (250 mg QD and 500 mg single dose) kinetics reported in the two DDI studies (Somogyi et al., 1987; Wang et al., 2008). A single virtual individual was used with the mean attributes of the healthy Caucasian (Somogyi et al., 1987) or Chinese (Wang et al., 2008) populations within the Simcyp Simulator.

3. Results

3.1. Initial model

A RAF of 3 for hepatic OCT1 uptake transport was determined on fitting the metformin training data. As expected, the scaled passive permeability of metformin across the apical and basal membranes of renal cells was negligible ($\text{CL}_{\text{PD}} = 4.26 \times 10^{-7} \text{ mL} \cdot \text{min}^{-1} \cdot 10^6 \text{ PTC}^{-1}$). This, combined with the fact that transporter mediated uptake and efflux were defined as unidirectional processes in the conventional model, meant that MATE1/2-K efflux had negligible impact on simulated plasma metformin concentrations. On this basis, plasma metformin concentrations were used to define a suitable value for the RAF for OCT2 uptake

whereas urinary excretion profiles were used to define a corresponding value for MATE1/2-K efflux. RAF values of 3 were determined for both metformin renal OCT2 uptake and MATE1/2-K efflux.

Simulated mean plasma metformin concentrations after single and BID oral doses of 500 mg metformin HCl and mean plasma AUC after single 500 to 1500 mg doses were consistent with observed values (Fig. 3A, B and D). Simulated mean C_{max} values were in agreement with observed values for 6 out of 7 studies, while simulated t_{max} values of 2 to 3 h were within 1 h of observed mean values (Supplementary Fig. 1). Simulated urinary recoveries of metformin were consistent with observed values, when the dose of free metformin base, bioavailability and fraction excreted in urine were considered (Fig. 3C). The simulated mean bioavailability and renal clearance values of 0.62 ± 0.10 and $32.0 \pm 9.0 \text{ L}\cdot\text{h}^{-1}$ (SD) in healthy subjects were consistent with observed values (Graham et al., 2011). The standard deviations of AUC, C_{max} , t_{max} and urinary recovery values from the simulated trials were consistent with observed values in 100, 67, 40 and 80% of cases, respectively (Supplementary Fig. 2).

Simulated mean plasma cimetidine concentrations after a single 300 mg oral dose only matched observed values from 3 h (Walkenstein et al., 1978); at earlier time points some individual profiles showed double peaks that were not recovered by the first-order absorption function (Fig. 4A). Nevertheless, the simulated mean (SD) AUC(0, 12 h) of $5.8 \pm 1.5 \text{ mg}\cdot\text{L}^{-1}\cdot\text{h}$ (SD) was comparable to the observed value of $5.0 \pm 1 \text{ mg}\cdot\text{L}^{-1}\cdot\text{h}$ (SD). Simulated mean plasma cimetidine concentrations during administration of 400 mg BID (Muirhead et al., 1986; Somogyi et al., 1981) and TID (Kirch et al., 1989) were consistent with observed values (Fig. 4B–C). The range of simulated urinary recoveries of unchanged cimetidine at 300 mg SD and 400 mg BID captured the observed values. However, an overprediction of the urinary recovery of cimetidine was evident at the 400 mg TID dose (Fig. 4D).

In the absence of cimetidine, the simulated mean plasma metformin AUC (0,24 h) of $7.1 \text{ mg}\cdot\text{L}^{-1}\cdot\text{h}$ (single 500 mg dose) was within 10% of the value of $6.6 \text{ mg}\cdot\text{L}^{-1}\cdot\text{h}$ observed by Wang et al. (2008); it was $3.3 \text{ mg}\cdot\text{L}^{-1}\cdot\text{h}$ (250 mg QD) compared to the value of $4.3 \text{ mg}\cdot\text{L}^{-1}\cdot\text{h}$ observed by Somogyi et al. (1987). In part, the latter discrepancy may be related to the inclusion in the study of Somogyi et al. of 2 subjects out of the 7 with GFR values of less than $40 \text{ mL}\cdot\text{min}^{-1}$. In the presence of cimetidine (400 mg BID), observed increases in metformin AUC and C_{max} values were 1.46- and 1.73-fold (Somogyi et al., 1987) and 1.46- and 1.40-fold (Wang et al., 2008), but the model predicted no change. While Somogyi et al. observed a non-significant 4% increase in the urinary recovery of metformin when co-administered with cimetidine, Wang et al. reported an overall 21% decrease (albeit not significant for OCT1 homozygous wild-type subjects). The model predicted no change in the urinary recovery of metformin in the presence of cimetidine.

Using a trial design matched to that of Somogyi et al. (1987), sensitivity analysis indicated that the observed metformin plasma AUC ratio could only be recovered when the cimetidine K_i value for OCT2 was decreased 1000-fold from the value of $124 \mu\text{M}$ observed *in vitro* (Ito et al., 2012). This was accompanied by a predicted decrease in the metformin concentration ratio (DDI/control) in the cells of the first segment of the proximal tubule from 1.8 to 0.6 but little change in the urinary recovery of unchanged metformin (Fig. 5A). Decreasing the cimetidine K_i for MATE1/2-K from the value determined *in vitro* of $5.4 \mu\text{M}$ had negligible impact on metformin plasma AUC and urinary recovery ratios although, as expected, metformin concentrations in the first segment of the proximal tubule were very sensitive to this parameter (Fig. 5B). The effect of decreasing the cimetidine K_i for OCT1 from its *in vitro* value of $104 \mu\text{M}$ on the metformin plasma AUC ratio was minimal, whereas simultaneously decreasing the cimetidine K_i values for OCT1 and OCT2 by

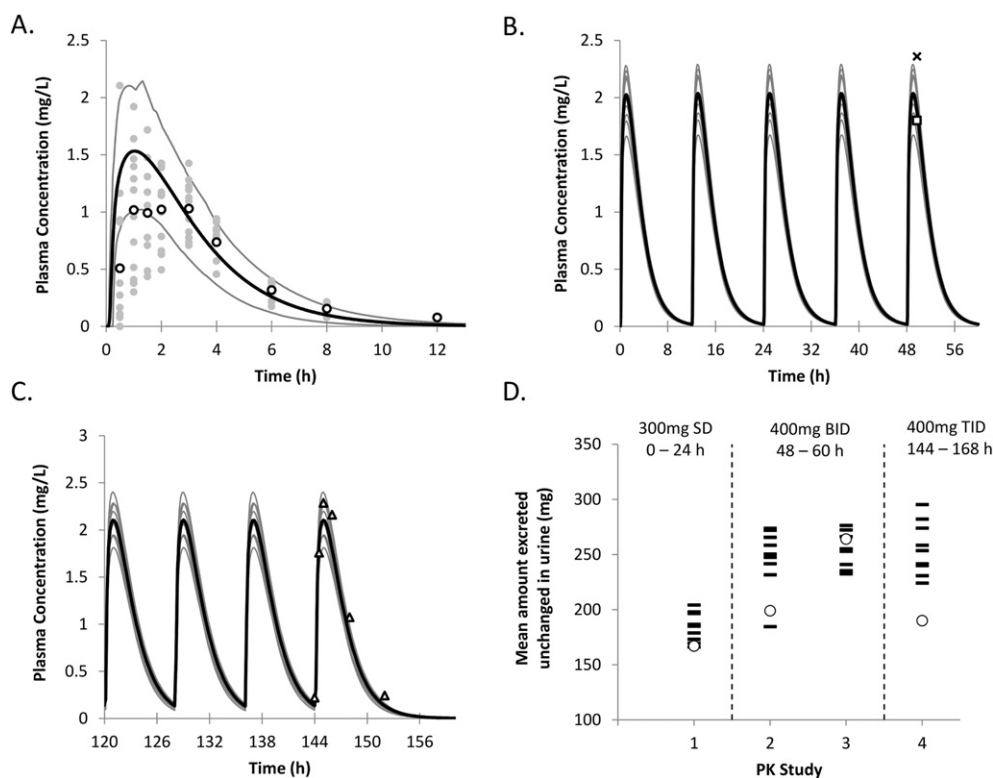


Fig. 4. Comparison of simulated and observed (A) plasma cimetidine concentrations after a single 300 mg dose (black and grey lines represent simulated mean and 95th percentiles, respectively, O and grey dots represent mean and individual data, respectively, from Walkenstein et al. (1978), (B) plasma cimetidine concentrations after 400 mg BID dosing (black and grey lines represent simulated overall and trial means, respectively, (X = Somogyi et al., 1987, □ = Muirhead et al., 1986), and (C) 400 mg TID dosing (black and grey lines represent simulated overall and trial means, respectively, (Δ = Kirch et al., 1989). Comparison of simulated (10 trials) (—) and observed (O) mean cimetidine AUC values (C) and urinary recovery of unchanged cimetidine (D). PK studies: 1, (Walkenstein et al., 1978); 2, (Muirhead et al., 1986); 3, (Somogyi et al., 1987); 4, (Kirch et al., 1989).

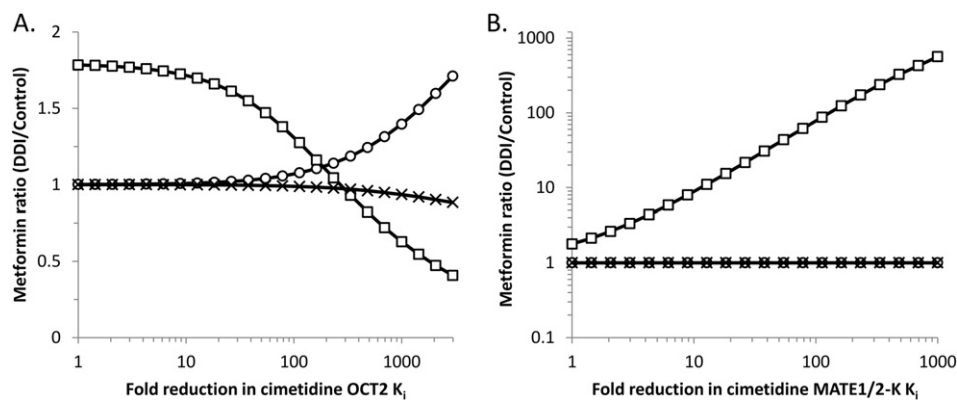


Fig. 5. Sensitivity of ratios (DDI/control) of metformin (O) plasma AUC, (□) proximal tubule cell segment 1 AUC and (X) urinary recovery to cimetidine K_i values for (A) OCT2, (B) MATE1/2-K and (C) both OCT1 and OCT2 based on a PBPK model incorporating a conventional description of transport kinetics for both drugs.

500-fold was necessary to recover the observed metformin plasma AUC ratio.

3.2. Model refinement

The electrogenic model of the transport of metformin by OCT2 was superior to the conventional model in describing uptake in transfected HEK293 cells, with a resulting J_{OCT2} estimate (SE) of $1155 \pm 158 \text{ pmol} \cdot \text{min}^{-1} \cdot \text{volt}^{-1} \cdot 10^6 \text{ cells}^{-1}$ (Fig. 6A). The corresponding model for OCT1 transport was able to recover the metformin uptake in transfected HEK293 cells reasonably well, with a J_{OCT1} estimate (SE) of $27.5 \pm 5.0 \text{ pmol} \cdot \text{min}^{-1} \cdot \text{volt}^{-1} \cdot 10^6 \text{ cells}^{-1}$ (Fig. 6B). However, in this case, the model did not provide an improvement over the conventional model.

Following the introduction of electrogenic functions for hepatic OCT1 transport and renal OCT2 transport into the metformin PBPK model, RAFs of 1.1, 2.3 and 1.0 were determined for OCT1, OCT2 and MATEs, respectively. While the incorporation of electrogenic OCT1 and OCT2 transport did not change the simulation of plasma drug concentrations in the absence of cimetidine, it did introduce sensitivity to MATE1/2-K inhibition (Fig. 7). To recover the full extent of the change in the plasma AUC of metformin in the presence of cimetidine it was necessary to invoke a 12-fold decrease in the cimetidine K_i for MATE1/2-K or a combined 8-fold decrease in the K_i 's for OCT1, OCT2 and MATE1/2-K (Somogyi et al., 1987 data, Fig. 8A). The corresponding decrease in K_i 's for OCT1, OCT2 and MATE1/2-K necessary to recover the observations from Wang et al. (2008) was 18-fold (Fig. 8B). The correlation of observed and simulated plasma metformin concentrations with

the initial and final models is provided in Supplementary Figs. 3 and 4, respectively.

4. Discussion

Incorporation of permeability-limited hepatic uptake by OCT1 and active renal transport by OCT2 and MATEs into a PBPK model allowed the simulation of plasma concentrations and urinary excretion of metformin when given alone. However, complete development of this PBPK model from the 'bottom up' was not possible, particularly in the absence of robust *in vitro* and *in vivo* abundance data for the relevant transporters. Therefore, it was necessary to fit *in vivo* data for metformin to derive net transporter scalars (RAFTs). The RAF of 3 for OCT1, OCT2 and MATE transport that was determined with the original metformin PBPK model compares to a value of 5.3 reported by Posada et al. (2015) for OAT3 mediated renal uptake of pemetrexed based on HEK293 cell data using a similar approach. A further issue with respect to metformin relates to its low passive permeability. While active uptake was assigned to the liver and the kidney, it was assumed that distribution into all other tissues was perfusion-limited. A marked time-dependence in the value of the blood/plasma concentration ratio of metformin, ranging from 0.5 at early times to 6 at later times in a representative subject after oral dosing (Tucker et al., 1981), indicates that general cellular penetration is slow or that uptake transporters operate more widely with respect to net distribution. In modelling the kinetics of metformin an average blood/plasma concentration ratio was used based on relative blood-to-plasma AUC values. Xie et al. (2015) recently reported a PBPK model for metformin in which the incorporation of plasma - blood cell distribution rate constants allowed recovery of

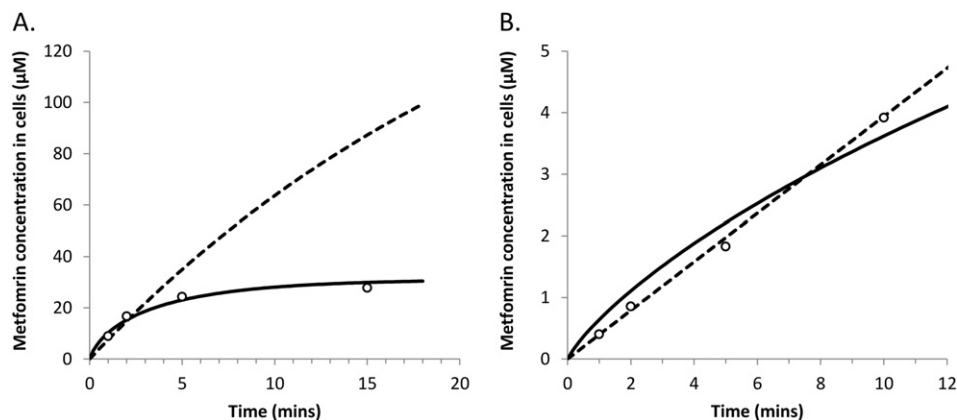


Fig. 6. Comparison of the ability of a conventional model (dashed lines) and an electrogenic model (solid line) to describe experimental data (open circles) on the uptake of metformin by (A) hOCT2 transfected HEK293 cells, (Kimura et al., 2005) or (B) hOCT1 transfected HEK293 cells, (Nies et al., 2011).

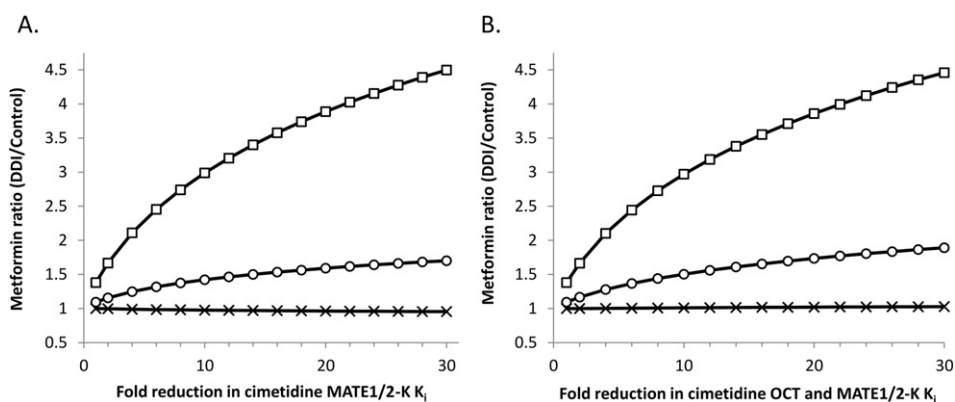


Fig. 7. Sensitivity of ratios (DDI/control) of metformin (O) plasma AUC, (□) proximal tubule cell segment 1 AUC and (X) urinary recovery to in cimetidine K_i for (A) MATE1/2-K and (B) OCT1, OCT2 and MATE1/2-K based on a PBPK model incorporating an electrochemical description of metformin OCT2 transport.

both plasma and whole blood drug concentrations over an extended time. When a blood cell distribution compartment was incorporated into the metformin PBPK model of the current study (using a similar approach to Xie et al.), simulated plasma metformin concentrations and the extent of the DDI with cimetidine were unaffected (data not shown). Therefore the approximation to an average blood/plasma concentration ratio used in the original model is not considered to detract from the main findings of this modelling exercise. *In vivo* data indicate that the oral absorption of metformin shows a degree of saturability (Proctor et al., 2008; Tucker et al., 1981). This would be consistent with the suggestion that the drug is subject to PMAT, OCT1 and OCT3 mediated uptake on the apical membrane of enterocytes, and that there is interplay between these uptake transporters and paracellular absorption (Proctor et al., 2008; Zhou et al., 2007). Although the PBPK model developed for metformin did not incorporate a saturable, transport-mediated component to oral absorption, it was able to recover plasma drug concentrations over the 500–1500 mg oral dose range with reasonable accuracy.

To simulate the effect of co-administration of cimetidine acting as an inhibitor of MATE and OCT transporters (Fig. 2), it was necessary to refine the original metformin PBPK model by introducing electrochemical modulation of OCT1 and OCT2 transport. *In vitro* studies have reported cimetidine K_i values between 21 and 94-fold lower for the inhibition of MATEs compared to OCTs, concluding that the inhibition of OCTs by cimetidine is unlikely at therapeutic doses (Ito et al., 2012; Tsuda et al., 2009). However, the conventional model of OCT transport is unidirectional and insensitive to intracellular substrate concentrations, and transcellular passive permeability of metformin is considered to be negligible. Under these conditions, inhibition of MATE1/2-K mediated

metformin efflux in the proximal tubule by cimetidine had no effect on simulated plasma metformin concentrations, despite a significant increase in drug concentration within the proximal tubule cells (Fig. 5B). This was clearly inconsistent with the observed 46% increase in plasma metformin AUC (Somogyi et al., 1987; Wang et al., 2008).

The OCTs function as electrogenic transporters, with both membrane potential and the substrate concentration gradient across the membrane providing the driving force for transport (Koepsell et al., 2007; Pelis and Wright, 2011). This combined electrochemical driving force allows a higher concentration of cations on one side of a membrane as they move down their electrochemical gradients, to a point that can be defined by their Nernst potentials. Data from rats indicate that Oct2 functions as a cation uniporter at low substrate concentrations, but as an electroneutral cation exchanger at high substrate concentrations on both sides of the membrane (Koepsell, 2011). Although well-known as a determinant of passive ion transport (Barts and Borst-Pauwels, 1985; Stein, 1977), this phenomenon is not accounted for in conventional models applied to the OCT mediated transport of drugs. In these conventional models, the rate of drug transport is defined as a first order process (Hsu et al., 2014) or by a Michaelis–Menten function when saturation is observed at higher substrate concentrations (Jamei et al., 2014; Neuhoff et al., 2013b). Although such models adequately describe the uptake of metformin *in vitro*, in which experiments are usually conducted over a time-course of several minutes, PBPK model simulations are applied over a significantly longer time-course of hours or days, requiring that the full impact of intracellular accumulation on OCT uptake be accounted for.

In the current study, the application of functions describing electrochemically-mediated OCT2 transport was able to account for a

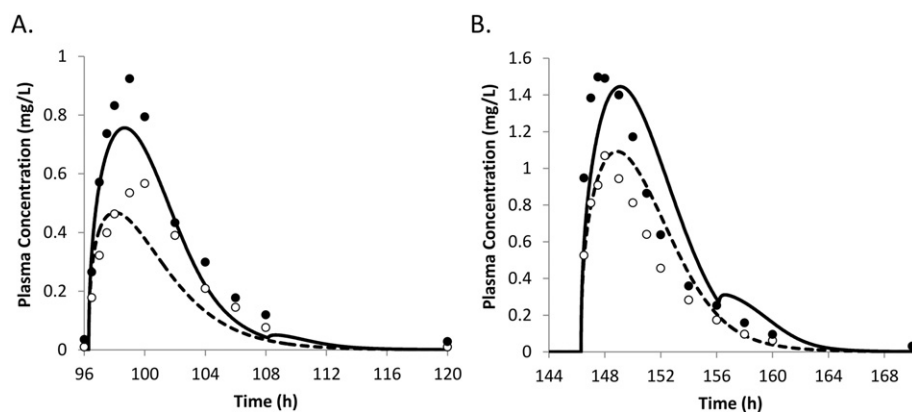


Fig. 8. Comparison of observed mean plasma metformin concentrations with (filled circles) and without (open circles) co-administration of cimetidine from (A) Somogyi et al. (1987) and (B) Wang et al. (2008) and corresponding simulated data with (solid line) and without (dashed line) co-administration of cimetidine. Simulations were performed for a population representative individual using the electrogenic OCT2 model and with cimetidine K_i's for OCT1, OCT2 and MATE1/2-K decreased by 8 and 16-fold from those determined *in vitro*.

decrease in the driving force for metformin uptake into OCT2 transfected HEK293 cells as its intracellular concentration increased, relative to that predicted by a conventional model. Incorporation of electrogenic models for OCT1 and OCT2 transport within the metformin PBPK model rendered the plasma concentrations of the drug sensitive to inhibition of renal MATE1/2-K by cimetidine, as the simulated increase in intracellular metformin concentrations led to a knock-on reduction in the OCT2 driving force. In combination with 8 to 18-fold decreases in the cimetidine K_i values for the relevant transporters from those measured *in vitro* and assuming the same net transporter uptake scalar (RAF) values as determined for metformin, it was possible to capture the change in metformin kinetics when co-administered with cimetidine. In contrast, using the conventional model, a 500-fold decrease in the *in vitro* OCT1 and OCT2 K_i estimates was required to simulate the metformin – cimetidine interaction.

An 8 to 18-fold decrease in transporter K_i values is consistent with other attempts to recover transporter-mediated DDIs for solute carriers (Greupink et al., 2013; Hsu et al., 2014; Li et al., 2014; Varma et al., 2012). This discrepancy may reflect inappropriate *in vitro* methodology or data analysis in the determination of K_i , or an incorrect assumption of competitive inhibition. The cimetidine K_i values used in the current study were obtained from *in vitro* experiments in which both OCT or MATE transporters were acting as uptake transporters (Ito et al., 2012). This means that the assumed concentration for inhibition (that applied to the incubation media) should be reasonably consistent with that at the transporter binding site. However, the MATE transporters could only be maintained in this orientation by applying a rich potassium ion concentration in the media, which may impact its function to an extent that the K_i estimate is inconsistent with its intrinsic value as an efflux transporter *in vivo*. Another factor to consider relates to the potential for MATE1 mediated efflux of metformin into bile. Although MATE1 is expressed on the canalicular membrane of human hepatocytes (Otsuka et al., 2005), the lack of detectable metformin in faeces after an intravenous dose and lack of secondary peaks precludes a clear role for this transporter in the liver, leading to its exclusion from our model (Pentikainen et al., 1979; Tucker et al., 1981). However, if MATE1 biliary efflux of metformin was found to be significant, its inhibition by cimetidine may contribute to the observed DDI. In light of these observations it is recommended to investigate a range of inhibitor K_i values (e.g. up to 20-fold lower than the *in vitro* value) when using the metformin model in prospective simulations with OCT/MATE transporter inhibitors.

Cimetidine is a weak inhibitor of CYP2D6 and CYP3A4 with K_i estimates of approximately 40 μM and 160 μM , respectively (Madeira et al., 2004; Martinez et al., 1999). As the metformin model included a minor metabolic clearance component, it is possible that inhibition of this component could contribute to the DDI. However, for CYP3A4, the enzyme which has shown evidence of metformin metabolism (Choi et al., 2010), this K_i estimate is 15-fold higher than the simulated maximum unbound concentration of cimetidine in the liver after 400 mg BID dosing. On this basis it is likely that any metabolic component to the observed DDI would be very minor. Although the clinical significance of the DDI between metformin and cimetidine is likely to be limited, this is not true of all DDIs involving renal OCT2 and MATE transport. The anticancer drug cisplatin is a substrate for OCT2, MATE1 and MATE2-K in the proximal tubule and its use is accompanied by a high risk of nephrotoxicity, linked to significant renal accumulation (Sprowl and Sparreboom, 2014). It has been suggested that cimetidine (Sprowl et al., 2013b) and erlotinib (Sprowl et al., 2013a) may protect against cisplatin induced nephrotoxicity through inhibition of OCT2. The current study highlights the potential impact of MATE1/2-K inhibition in this setting, and a role for PBPK modelling in clarifying the underlying processes. The coadministration of the OCT1 inhibitor verapamil has been associated with a decrease to the glucose lowering effect of metformin in the absence of significant changes in its plasma concentration or urinary excretion (Cho et al., 2014). This indicates the need for

further elaboration of the PBPK model for metformin that accounts for pharmacodynamics changes mediated through the modification of transport affecting access of the drug to sites of action in both liver and gut (Gong et al., 2012; McCreight et al., 2016).

5. Conclusion

We believe that, while highlighting some significant deficiencies in currently available data, the PBPK model that we have developed for metformin with electrochemical modulation of the rate of hepatic uptake by OCT1 and renal uptake by OCT2 moves forward understanding of the use of this compound as a model substrate for predicting OCT and MATE mediated DDIs.

Disclosures

HB, SN, LA, GL, HM, MJ, ARH and KRY are employed by Simcyp Ltd. (a Certara company). GT is a co-founder and advisor to Simcyp Ltd. (a Certara company).

Acknowledgements

The assistance of Eleanor Savill in preparing this manuscript is appreciated. The authors are grateful to Ming Zheng and Zheng Yang of Bristol Myers Squibb for useful discussion on metformin.

Appendix A. Supplementary data.

Supplementary data to this article can be found online at <http://dx.doi.org/10.1016/j.ejps.2016.03.020>.

References

- Avdeef, A., 2012. *Absorption and Drug Development: Solubility, Permeability, and Charge State*. second ed. Wiley-Interscience New Jersey.
- Avdeef, A., Berger, C.M., 2001. pH-metric solubility. 3. Dissolution titration template method for solubility determination. *European Journal of Pharmaceutical Sciences: Official Journal of the European Federation for Pharmaceutical Sciences* 14, pp. 281–291.
- Balan, G., Timmins, P., Greene, D.S., Marathe, P.H., 2001. In vitro-in vivo correlation (IVIVC) models for metformin after administration of modified-release (MR) oral dosage forms to healthy human volunteers. *J. Pharm. Sci.* 90, 1176–1185.
- Balimane, P.V., Chong, S., 2008. Evaluation of permeability and P-glycoprotein interactions: industry outlook. In: Krishna, R., Yu, L. (Eds.), *Biopharmaceutics Applications in Drug Development*. Springer, New York.
- Barts, P.W.J.A., Borst-Pauwels, G.W.F.H., 1985. Effects of membrane potential and surface potential on the kinetics of solute transport. *Biochim. Biophys. Acta* 813, 51–60.
- Caille, G., Lacasse, Y., Raymond, M., Landriault, H., Perrotta, M., Picirilli, G., Thiffault, J., Spenard, J., 1993. Bioavailability of metformin in tablet form using a new high pressure liquid chromatography assay method. *Biopharm. Drug Dispos.* 14, 257–263.
- Chemin, J., Monteil, A., Briquaire, C., Richard, S., Perez-Reyes, E., Nargeot, J., Lory, P., 2000. Overexpression of T-type calcium channels in HEK-293 cells increases intracellular calcium without affecting cellular proliferation. *FEBS Lett.* 478, 166–172.
- Chen, Y., Li, S., Brown, C., Cheatham, S., Castro, R.A., Leabman, M.K., Urban, T.J., Chen, L., Yee, S.W., Choi, J.H., Huang, Y., Brett, C.M., Burchard, E.G., Giacomini, K.M., 2009. Effect of genetic variation in the organic cation transporter 2 on the renal elimination of metformin. *Pharmacogenet. Genomics* 19, 497–504.
- Cho, S.K., Kim, C.O., Park, E.S., Chung, J.Y., 2014. Verapamil decreases the glucose-lowering effect of metformin in healthy volunteers. *Br. J. Clin. Pharmacol.* 78, 1426–1432.
- Choi, Y.H., Lee, U., Lee, B.K., Lee, M.G., 2010. Pharmacokinetic interaction between itraconazole and metformin in rats: competitive inhibition of metabolism of each drug by each other via hepatic and intestinal CYP3A1/2. *Br. J. Pharmacol.* 161, 815–829.
- Ding, Y., Jia, Y., Song, Y., Lu, C., Li, Y., Chen, M., Wang, M., Wen, A., 2014. The effect of lansoprazole, an OCT inhibitor, on metformin pharmacokinetics in healthy subjects. *Eur. J. Clin. Pharmacol.* 70, 141–146.
- Durant, G.J., Emmett, J.C., Ganellin, C.R., 1977. The chemical origin and properties of histamine H₂-receptor antagonists. In: Burland, W.L., Simkins, M.A. (Eds.), *Proceedings of the Second International Symposium on Histamine H₂ Receptor Antagonists*. Excerpta Medica, Oxford, pp. 1–12.
- Erdman, A.R., Mangravite, L.M., Urban, T.J., Lagpagan, L.L., Castro, R.A., de la Cruz, M., Chan, W., Huang, C.C., Johns, S.J., Kawamoto, M., Stryke, D., Taylor, T.R., Carlson, E.J., Ferrin, T.E., Brett, C.M., Burchard, E.G., Giacomini, K.M., 2006. The human organic anion transporter 3 (OAT3; SLC22A8): genetic variation and functional genomics. *American journal of physiology. Ren. physiol.* 290, F905–F912.

- Gillen, C.M., Forbush 3rd, B., 1999. Functional interaction of the K-Cl cotransporter (KCC1) with the Na-K-Cl cotransporter in HEK-293 cells. *Am. J. Phys.* 276, C328–C336.
- Gong, L., Goswami, S., Giacomini, K.M., Altman, R.B., Klein, T.E., 2012. Metformin pathways: pharmacokinetics and pharmacodynamics. *Pharmacogenet. Genomics* 22, 820–827.
- Graham, G.G., Punt, J., Arora, M., Day, R.O., Doogue, M.P., Duong, J.K., Furlong, T.J., Greenfield, J.R., Greenup, L.C., Kirkpatrick, C.M., Ray, J.E., Timmins, P., Williams, K.M., 2011. Clinical pharmacokinetics of metformin. *Clin. Pharmacokinet.* 50, 81–98.
- Grahnén, A., von Bahr, C., Lindström, B., Rosen, A., 1979. Bioavailability and pharmacokinetics of cimetidine. *Eur. J. Clin. Pharmacol.* 16, 335–340.
- Greupink, R., Schreurs, M., Benne, M.S., Huisman, M.T., Russel, F.G., 2013. Semi-mechanistic physiologically-based pharmacokinetic modeling of clinical glibenclamide pharmacokinetics and drug–drug-interactions. *European Journal of Pharmaceutical Sciences: Official Journal of the European Federation for Pharmaceutical Sciences* 49, pp. 819–828.
- Grun, B., Kiessling, M.K., Burhenne, J., Riedel, K.D., Weiss, J., Rauch, G., Haefeli, W.E., Czock, D., 2013. Trimethoprim-metformin interaction and its genetic modulation by OCT2 and MATE1 transporters. *Br. J. Clin. Pharmacol.* 76, 787–796.
- Gugler, R., Somogyi, A., K.v., B., 1981b. The biliary excretion of histamine H₂-receptor antagonists cimetidine and omeprazole. *Clin. Pharmacol. Ther.* 29, 249.
- Gugler, R., Brand, M., Somogyi, A., 1981a. Impaired cimetidine absorption due to antacids and metoclopramide. *Eur. J. Clin. Pharmacol.* 20, 225–228.
- Gusler, G., Gorsline, J., Levy, G., Zhang, S.Z., Weston, I.E., Naret, D., Berner, B., 2001. Pharmacokinetics of metformin gastric-retentive tablets in healthy volunteers. *J. Clin. Pharmacol.* 41, 655–661.
- Harwood, M.D., Neuhoff, S., Carlson, G.L., Warhurst, G., Rostami-Hodjegan, A., 2013. Absolute abundance and function of intestinal drug transporters: a prerequisite for fully mechanistic in vitro-in vivo extrapolation of oral drug absorption. *Biopharm. Drug Dispos.* 34, 2–28.
- Hsu, V., Vieira, M.d.L.T., Zhao, P., Zhang, L., Zheng, J.H., Nordmark, A., Berglund, E.G., Giacomini, K.M., Huang, S.M., 2014. Towards quantitation of the effects of renal impairment and probenecid inhibition on kidney uptake and efflux transporters, using physiologically based pharmacokinetic modelling and simulations. *Clin. Pharmacokinet.* 53, 283–293.
- Ito, S., Kusuhara, H., Kuroiwa, Y., Wu, C., Moriyama, Y., Inoue, K., Kondo, T., Yuasa, H., Nakayama, H., Horita, S., Sugiyama, Y., 2010. Potent and specific inhibition of mMate1-mediated efflux of type I organic cations in the liver and kidney by pyrimethamine. *J. Pharmacol. Exp. Ther.* 333, 341–350.
- Ito, S., Kusuhara, H., Yokochi, M., Toyoshima, J., Inoue, K., Yuasa, H., Sugiyama, Y., 2012. Competitive inhibition of the luminal efflux by multidrug and toxin extrusions, but not basolateral uptake by organic cation transporter 2, is the likely mechanism underlying the pharmacokinetic drug–drug interactions caused by cimetidine in the kidney. *J. Pharmacol. Exp. Ther.* 340, 393–403.
- Jamei, M., Bajot, F., Neuhoff, S., Barter, Z., Yang, J., Rostami-Hodjegan, A., Rowland-Yeo, K., 2014. A mechanistic framework for in vitro-in vivo extrapolation of liver membrane transporters: prediction of drug–drug interaction between rosuvastatin and cyclosporine. *Clin. Pharmacokinet.* 53, 73–87.
- Johansson, S., Read, J., Oliver, S., Steinberg, M., Li, Y., Lisbon, E., Mathews, D., Leese, P.T., Martin, P., 2014. Pharmacokinetic evaluations of the co-administrations of vandetanib and metformin, digoxin, midazolam, omeprazole or ranitidine. *Clin. Pharmacokinet.* 53, 837–847.
- Karttunen, P., Uusitupa, M., Lammisvuo, U., 1983. The pharmacokinetics of metformin: a comparison of the properties of a rapid-release and a sustained-release preparation. *Int. J. Clin. Pharmacol. Ther. Toxicol.* 21, 31–36.
- Kimura, N., Okuda, M., Inui, K., 2005. Metformin transport by renal basolateral organic cation transporter hOCT2. *Pharm. Res.* 22, 255–259.
- Kirch, W., Janisch, H.D., Ohnhaus, E.E., van Peer, A., 1989. Cisapride-cimetidine interaction: enhanced cisapride bioavailability and accelerated cimetidine absorption. *Ther. Drug Monit.* 11, 411–414.
- Koepsell, H., 2011. Substrate recognition and translocation by polyspecific organic cation transporters. *Biol. Chem.* 392, 95–101.
- Koepsell, H., Lips, K., Volk, C., 2007. Polyspecific organic cation transporters: structure, function, physiological roles, and biopharmaceutical implications. *Pharm. Res.* 24, 1227–1251.
- Kusuhara, H., Ito, S., Kumagai, Y., Jiang, M., Shiroshita, T., Moriyama, Y., Inoue, K., Yuasa, H., Sugiyama, Y., 2011. Effects of a MATE protein inhibitor, pyrimethamine, on the renal elimination of metformin at oral microdose and at therapeutic dose in healthy subjects. *Clin. Pharmacol. Ther.* 89, 837–844.
- Lazorova, L., 2010. Personal Communication. Uppsala University, Sweden, Dept of Pharmacy.
- Lebert, P.A., Mahon, W.A., MacLeod, S.M., Soldin, S.J., Fenje, P., Vandenberghe, H.M., 1981. Ranitidine kinetics and dynamics II. Intravenous dose studies and comparison with cimetidine. *Clin. Pharmacol. Ther.* 30, 545–550.
- Li, R., Barton, H.A., Varma, M.V., 2014. Prediction of pharmacokinetics and drug–drug interactions when hepatic transporters are involved. *Clin. Pharmacokinet.* 53, 659–678.
- Madeira, M., Levine, M., Chang, T.K., Mirfazaelian, A., Bellward, G.D., 2004. The effect of cimetidine on dextromethorphan O-demethylase activity of human liver microsomes and recombinant CYP2D6. *Drug Metab. Dispos.* 32, 460–467.
- Martinez, C., Albet, C., Agundez, J.A., Herrero, E., Carrillo, J.A., Marquez, M., Benitez, J., Ortiz, J.A., 1999. Comparative in vitro and in vivo inhibition of cytochrome P450 CYP1A2, CYP2D6, and CYP3A by H₂-receptor antagonists. *Clin. Pharmacol. Ther.* 65, 369–376.
- Matsumoto, T., Kanamoto, T., Otsuka, M., Omote, H., Moriyama, Y., 2008. Role of glutamate residues in substrate recognition by human MATE1 polyspecific H⁺/organic cation exporter. *American journal of physiology. Cell. Physiol.* 294, C1074–C1078.
- McCreight, L.J., Bailey, C.J., Pearson, E.R., 2016. Metformin and the gastrointestinal tract. *Diabetologia* 59, 426–435.
- Muirhead, M.R., Somogyi, A.A., Rolan, P.E., Bochner, F., 1986. Effect of cimetidine on renal and hepatic drug elimination: studies with triamterene. *Clin. Pharmacol. Ther.* 40, 400–407.
- Muller, J., Lips, K.S., Metzner, L., Neubert, R.H., Koepsell, H., Brandsch, M., 2005. Drug specificity and intestinal membrane localization of human organic cation transporters (OCT). *Biochem. Pharmacol.* 70, 1851–1860.
- Neuhoff, S., Gaohua, L., Burt, H., Jamei, M., Li, L., Tucker, G.T., Rostami-Hodjegan, A., 2013a. Accounting for transporters in renal clearance: towards a mechanistic kidney model (Mech KiM). In: Steffansen, B. (Ed.), *Transporters in Drug Development* Springer, New York, pp. 155–177.
- Neuhoff, S., Yeo, K.R., Barter, Z., Jamei, M., Turner, D.B., Rostami-Hodjegan, A., 2013b. Application of permeability-limited physiologically-based pharmacokinetic models: part I-digoxin pharmacokinetics incorporating P-glycoprotein-mediated efflux. *J. Pharm. Sci.* 102, 3145–3160.
- Nies, A.T., Hofmann, U., Resch, C., Schaeffeler, E., Rius, M., Schwab, M., 2011. Proton pump inhibitors inhibit metformin uptake by organic cation transporters (OCTs). *PLoS One* 6, e22163.
- Ohta, K.Y., Inoue, K., Yasujima, T., Ishimaru, M., Yuasa, H., 2009. Functional characteristics of two human MATE transporters: kinetics of cimetidine transport and profiles of inhibition by various compounds. *Journal of Pharmacy & Pharmaceutical Sciences: a Publication of the Canadian Society for Pharmaceutical Sciences, Societe canadienne des sciences pharmaceutiques* 12, pp. 388–396.
- Otsuka, M., Matsumoto, T., Morimoto, R., Arioka, S., Omote, H., Moriyama, Y., 2005. A human transporter protein that mediates the final excretion step for toxic organic cations. *Proc. Natl. Acad. Sci. U. S. A.* 102, 17923–17928.
- Park, M.T., Lee, M.S., Kim, S.H., Jo, E.C., Lee, G.M., 2004. Influence of culture passages on growth kinetics and adenovirus vector production for gene therapy in monolayer and suspension cultures of HEK 293 cells. *Appl. Microbiol. Biotechnol.* 65, 553–558.
- Pelis, R.M., Wright, S.H., 2011. Renal transport of organic anions and cations. *Compr Physiol* 1, 1795–1835.
- Pentikainen, P.J., 1986. Bioavailability of metformin. comparison of solution, rapidly dissolving tablet, and three sustained release products. *Int. J. Clin. Pharmacol. Ther. Toxicol.* 24, 213–220.
- Pentikainen, P.J., Neuvonen, P.J., Penttila, A., 1979. Pharmacokinetics of metformin after intravenous and oral administration to man. *Eur. J. Clin. Pharmacol.* 16, 195–202.
- Posada, M.M., Bacon, J.A., Schneck, K.B., Tirona, R.G., Kim, R.B., Higgins, J.W., Pak, Y.A., Hall, S.D., Hillgren, K.M., 2015. Prediction of renal transporter mediated drug–drug interactions for pemetrexed using physiologically based pharmacokinetic modeling. *Drug Metabolism and Disposition: the Biological Fate of Chemicals* 43, pp. 325–334.
- Proctor, W.R., Bourdet, D.L., Thakker, D.R., 2008. Mechanisms underlying saturable intestinal absorption of metformin. *Drug Metabolism and Disposition: the Biological Fate of Chemicals* 36, pp. 1650–1658.
- Ray, P., 1961. Complex compounds of biguanides and guanylureas with metallic elements. *Chem. Rev.* 61, 313–359.
- Robert, F., Fendri, S., Hary, L., Lacroix, C., Andrejak, M., Lalau, J.D., 2003. Kinetics of plasma and erythrocyte metformin after acute administration in healthy subjects. *Diabetes Metab.* 29, 279–283.
- Rodgers, T., Rowland, M., 2007. Mechanistic approaches to volume of distribution predictions: understanding the processes. *Pharm. Res.* 24, 918–933.
- Sambol, N.C., Chiang, J., Lin, E.T., Goodman, A.M., Liu, C.Y., Benet, L.Z., Cogan, M.G., 1995. Kidney function and age are both predictors of pharmacokinetics of metformin. *J. Clin. Pharmacol.* 35, 1094–1102.
- Sambol, N.C., Brookes, L.G., Chiang, J., Goodman, A.M., Lin, E.T., Liu, C.Y., Benet, L.Z., 1996a. Food intake and dosage level, but not tablet vs solution dosage form, affect the absorption of metformin HCl in man. *Br. J. Clin. Pharmacol.* 42, 510–512.
- Sambol, N.C., Chiang, J., O'Conner, M., Liu, C.Y., Lin, E.T., Goodman, A.M., Benet, L.Z., Karam, J.H., 1996b. Pharmacokinetics and pharmacodynamics of metformin in healthy subjects and patients with noninsulin-dependent diabetes mellitus. *J. Clin. Pharmacol.* 36, 1012–1021.
- Schafer, G., Bojanowski, D., 1972. Interaction of biguanides with mitochondrial and synthetic membranes. *European journal of biochemistry/FEBS* 27, 364–375.
- Scheen, A.J., de Magalhães, A.C., Salvatore, T., Lefebvre, P.J., 1994. Reduction of the acute bioavailability of metformin by the alpha-glucosidase inhibitor acarbose in normal man. *Eur. J. Clin. Investig.* 24 (Suppl. 3), 50–54.
- Sirtori, C.R., Franceschini, G., Galli-Kienle, M., Cighetti, G., Galli, G., Bondioli, A., Conti, F., 1978. Disposition of metformin (N,N-dimethylbiguanide) in man. *Clin. Pharmacol. Ther.* 24, 683–693.
- Sogame, Y., Kitamura, A., Yabuki, M., Komuro, S., 2009. A comparison of uptake of metformin and phenformin mediated by hOCT1 in human hepatocytes. *Biopharm. Drug Dispos.* 30, 476–484.
- Somogyi, A., Gugler, R., 1985. Effect of variations in urine pH and flow rate on cimetidine renal disposition in man. *Biopharm. Drug Dispos.* 6, 345–349.
- Somogyi, A., Rohner, H.G., Gugler, R., 1980. Pharmacokinetics and bioavailability of cimetidine in gastric and duodenal ulcer patients. *Clin. Pharmacokinet.* 5, 84–94.
- Somogyi, A., Thielscher, S., Gugler, R., 1981. Influence of phenobarbital treatment on cimetidine kinetics. *Eur. J. Clin. Pharmacol.* 19, 343–347.
- Somogyi, A., Stockley, C., Keal, J., Rolan, P., Bochner, F., 1987. Reduction of metformin renal tubular secretion by cimetidine in man. *Br. J. Clin. Pharmacol.* 23, 545–551.
- Sprowl, J.A., Sparreboom, A., 2014. Uptake carriers and oncology drug safety. *Drug Metabolism and Disposition: the Biological Fate of Chemicals* 42, pp. 611–622.
- Sprowl, J.A., Mathijssen, R.H., Sparreboom, A., 2013a. Can erlotinib ameliorate cisplatin-induced toxicities? *J. Clin. Oncol.* 31, 3442–3443.
- Sprowl, J.A., van Doorn, L., Hu, S., van Gerven, L., de Bruijn, P., Li, L., Gibson, A.A., Mathijssen, R.H., Sparreboom, A., 2013b. Conjointive therapy of cisplatin with the OCT2 inhibitor cimetidine: influence on antitumor efficacy and systemic clearance. *Clin. Pharmacol. Ther.* 94, 585–592.

- Stein, W.D., 1977. How the kinetic parameters of the simple carrier are affected by an applied voltage. *Biochim. Biophys. Acta* 467, 376–385.
- Tahara, H., Kusuhashi, H., Endou, H., Koepsell, H., Imaoka, T., Fuse, E., Sugiyama, Y., 2005. A species difference in the transport activities of H2 receptor antagonists by rat and human renal organic anion and cation transporters. *J. Pharmacol. Exp. Ther.* 315, 337–345.
- Tamai, I., Yabuuchi, H., Nezu, J., Sai, Y., Oku, A., Shimane, M., Tsuji, A., 1997. Cloning and characterization of a novel human pH-dependent organic cation transporter, OCTN1. *FEBS Lett.* 419, 107–111.
- Taylor, D.C., Cresswell, P.R., Bartlett, D.C., 1978. The metabolism and elimination of cimetidine, a histamine H2-receptor antagonist, in the rat, dog, and man. *Drug Metabolism and Disposition: the Biological Fate of Chemicals* 6, pp. 21–30.
- Tsuda, M., Terada, T., Ueba, M., Sato, T., Masuda, S., Katsura, T., Inui, K., 2009. Involvement of human multidrug and toxin extrusion 1 in the drug interaction between cimetidine and metformin in renal epithelial cells. *J. Pharmacol. Exp. Ther.* 329, 185–191.
- Tucker, G.T., Casey, C., Phillips, P.J., Connor, H., Ward, J.D., Woods, H.F., 1981. Metformin kinetics in healthy subjects and in patients with diabetes mellitus. *Br. J. Clin. Pharmacol.* 12, 235–246.
- Tzvetkov, M.V., Vormfelde, S.V., Balen, D., Meineke, I., Schmidt, T., Sehart, D., Sabolic, I., Koepsell, H., Brockmoller, J., 2009. The effects of genetic polymorphisms in the organic cation transporters OCT1, OCT2, and OCT3 on the renal clearance of metformin. *Clin. Pharmacol. Ther.* 86, 299–306.
- U.S. Department of Health and Human Services, Food and Drug Administration, Center for Drug Evaluation and Research, 2012g. *Guidance for Industry: Drug Interactions Studies – Study Design, Data Analysis, Implications for Dosing, and Labeling Recommendations*. FDA, Silver Spring, MD.
- Varma, M.V., Lai, Y., Feng, B., Litchfield, J., Goosen, T.C., Bergman, A., 2012. Physiologically based modeling of pravastatin transporter-mediated hepatobiliary disposition and drug–drug interactions. *Pharm. Res.* 29, 2860–2873.
- Veech, R.L., Kashiwaya, Y., King, M.T., 1995. The resting membrane potential of cells are measures of electrical work, not of ionic currents. *Integr. Physiol. Behav. Sci.* 30, 283–307.
- Villeneuve, J.P., Fortunet-Fouin, H., Arsene, D., 1983. Cimetidine kinetics and dynamics in patients with severe liver disease. *Hepatology* 3, 923–927.
- Walkenstein, S.S., Dubb, J.W., Randolph, W.C., Westlake, W.J., Stote, R.M., Intocchia, A.P., 1978. Bioavailability of cimetidine in man. *Gastroenterology* 74, 360–365.
- Wang, Z.J., Yin, O.Q., Tomlinson, B., Chow, M.S., 2008. OCT2 polymorphisms and in-vivo renal functional consequence: studies with metformin and cimetidine. *Pharmacogenet. Genomics* 18, 637–645.
- Xie, F., Ke, A.B., Bowers, G.D., Zamek-Gliszczynski, M.J., 2015. Metformin's intrinsic blood-to-plasma partition ratio (B/P): reconciling the perceived high in vivo B/P > 10 with the in vitro equilibrium value of unity. *J. Pharmacol. Exp. Ther.* 354, 225–229.
- Zhou, M., Xia, L., Wang, J., 2007. Metformin transport by a newly cloned proton-stimulated organic cation transporter (plasma membrane monoamine transporter) expressed in human intestine. *Drug Metabolism and Disposition: the Biological Fate of Chemicals* 35, pp. 1956–1962.
- Zong, J., Borland, J., Jerva, F., Wynne, B., Choukour, M., Song, I., 2014. The effect of dolutegravir on the pharmacokinetics of metformin in healthy subjects. *J. Int. AIDS Soc.* 17, 19584.